

Using Transcripts for Nonparametric Monitoring of Serial Dependence

Christian H. Weiß*[†] José M. Amigó^{‡§}

May 27, 2026

Abstract

Control charts for process monitoring are widely used in practice. Most control charts require the monitored (residuals) process to be serially independent (and to satisfy specified distributional assumptions), whereas undetected dependence (or violations of distributional assumptions) may severely affect the charts' performances. Therefore, (distribution-free) control charts for monitoring serial dependence are of utmost relevance for practice. Recently, various nonparametric control charts have been proposed for this purpose, which are based on ordinal patterns, and which showed an appealing performance in detecting different types of serial dependence. In this research, we further progress in this direction and develop novel nonparametric control charts being based on transcripts and algebraic distances (as derived from ordinal patterns). The performance of the newly proposed control charts is evaluated in a simulation study, and their application in practice is illustrated with a real-world data example from chemical industry.

KEY WORDS: nonparametric control charts; ordinal patterns; self-starting control charts; serial dependence; nonlinear time series; transcripts.

1 Introduction

Since their proposal by Walter A. Shewhart more than 100 years ago (see Olmstead, 1967 for historical aspects), control charts received an enormous research interest and have been widely applied in practice in order to monitor a process $(X_t) = (X_t)_{t \in \mathbb{N} = \{1, 2, \dots\}}$ for possible process changes; see Montgomery (2009) for an overview. More precisely, a control chart can be understood as a sequential hypothesis test, with the in-control (IC) model

*Department of Mathematics and Statistics, Helmut Schmidt University, 22043 Hamburg, Germany

[†]Corresponding author. E-Mail: weissc@hsu-hh.de. ORCID: 0000-0001-8739-6631.

[‡]Centro de Investigación Operativa, Universidad Miguel Hernández, 03202 Elche, Spain

[§]E-Mail: jm.amigo@umh.es. ORCID: 0000-0002-1642-1171.

constituting the null hypothesis. If the process (X_t) experiences a change at some time $\tau \in \mathbb{N}$ (referred to as the change point), then it turns into an out-of-control (OOC) state (alternative hypothesis), the timely detection of which being the aim of statistical process monitoring (SPM). The vast majority of control charts that have been proposed so far (see Montgomery (2009) for references) assume that the monitored process is serially independent under IC-conditions; see Chakraborti & Sparks (2020) for a discussion. However, if this assumption is violated, it is well known since Alwan (1992) and Wardell et al. (1992) that the control chart's performance might be severely affected. Therefore, having a control chart that monitors the IC-assumption of serial dependence is crucial for practice. An analogous conclusion applies to the case of time-series monitoring, where control charts are typically applied to a residual series, which is serially uncorrelated under IC-conditions (Yourstone & Montgomery, 1989; Atienza et al., 1997).

In real-world applications, the monitored process (X_t) often does not follow a standard parametric distribution (such as the normal distribution). Hence, if the chart design relies on inappropriate distributional assumptions, the chart may exhibit an unexpected performance (such as frequent false alarms under IC-conditions or detection delays under OOC-conditions); see Chakraborti & Sparks (2020) for a discussion. This motivates the use of nonparametric (distribution-free) control charts as recently surveyed by Chakraborti & Graham (2019) and Koutras & Triantafyllou (2020), which show the same performance irrespective of the actual marginal distribution of (X_t) . Recently, Weiß & Testik (2023) developed a bunch of nonparametric control charts that monitor for serial dependence in (X_t) . While these charts are designed for continuously distributed processes (X_t) , with arbitrary marginal distribution and being independent and identically distributed (i. i. d.) under IC-conditions, they can also be applied to discrete-valued processes (such as a count process) if additional jittering (Machado & Santos Silva, 2005) is used (e. g., if i. i. d. uniform noise with range $(0; 1)$ is added to a count process, see Weiß & Schnurr, 2024). Thus, without loss of generality, let us focus on continuously distributed processes (X_t) in the sequel, which are assumed to be i. i. d. under IC-conditions.

The nonparametric control charts for serial dependence developed by Weiß & Testik (2023) combine so-called ordinal patterns (OPs) with an exponentially weighted moving-average (EWMA) approach; see Section 2 for a detailed review. In a recent research on nonparametric hypothesis tests for serial dependence by Weiß & Amigó (2026), however, it was shown that superior power is often achieved if the test statistics do not rely on ordinary OPs, but if so-called transcripts (and possibly related algebraic distances) are considered instead. Therefore, in the present research, we develop novel nonparametric control charts being based on the transcripts computed from (X_t) , and we compare their performance to the former OP-based control

charts of Weiß & Testik (2023). The relevant background on transcripts and algebraic distances is provided by Section 3, and our novel transcript-based control charts are introduced in Section 4. Their performance, evaluated in terms of the average run length (ARL) under IC- or OOC-conditions, is investigated by simulations in Section 5, while an illustrative data example from chemical industry is presented in Section 6. A summary, the main conclusions, and an outlook are the contents of the final Section 7.

2 Review: Control Charts based on Ordinal Patterns

The idea to compute OPs from a real-valued and continuously distributed process (X_t) dates back to Bandt & Pompe (2002). Let $m \in \mathbb{N} = \{1, 2, \dots\}$ with $m \geq 2$ be the length of the considered OPs, and let S_m denote the symmetric group of degree m , which consists of the $m!$ possible permutations of the integers $\{1, \dots, m\}$ endowed with function composition. The permutations $\pi \in S_m = \{\pi^{[1]}, \dots, \pi^{[m!]} \}$ can be used in various ways to represent the $m!$ different OPs of a vector $\mathbf{x} = (x_1, \dots, x_m) \in \mathbb{R}^m$, see Berger et al. (2019) for a discussion. In what follows, we focus on the *permutation representation*, where $\pi = (i_1, \dots, i_m) \in S_m$ expresses that permutation, which causes an ascending order of the components of \mathbf{x} :

$$x_{i_1} \leq x_{i_2} \leq \dots \leq x_{i_m}, \quad \text{and} \quad i_{k-1} < i_k \text{ if } x_{i_{k-1}} = x_{i_k} \text{ for } k \geq 2. \quad (1)$$

The second case in (1) accounts for the possible occurrence of ties in \mathbf{x} . As (X_t) is continuously distributed, ties happen with probability zero. However, due to the limited measurement accuracy in real-world applications, ties may happen anyway, but we assume that they occur at an negligible rate.

By continuously mapping the segments $\mathbf{X}_t = (X_t, \dots, X_{t+m-1})$ of the process (X_t) onto its corresponding OP π_t , for $t = 1, 2, \dots$, the originally real-valued process (X_t) is discretized and transformed into the OP-series $(\pi_t) = (\pi_t)_{t \in \mathbb{N}}$ in an online manner. According to the proposal by Weiß & Testik (2023), the process (X_t) is now monitored by monitoring its corresponding OP-series (π_t) . If the original process (X_t) runs under IC-conditions, i. e., if it is i. i. d., then the OP-series (π_t) is stationary with a discrete-uniform marginal distribution, irrespective of the actual marginal distribution of (X_t) . Hence, its $m!$ -dimensional probability mass function (PMF) vector $\mathbf{p}_\pi = (p_{\pi,1}, \dots, p_{\pi,m!})^\top$ with $p_{\pi,k} = P(\pi_t = \pi^{[k]})$ is equal to $\mathbf{p}_\pi^{(0)} = (1/m!, \dots, 1/m!)$. Deviations between \mathbf{p}_π and $\mathbf{p}_\pi^{(0)}$, in turn, indicate the presence of serial dependence in (X_t) .

More precisely, Weiß & Testik (2023) solely focused on OPs of length $m = 3$, which is indeed the most common choice in practice, see Bandt (2019). Then, the six possible OPs (in lexicographic order) can be summarized as

follows:

$$\begin{array}{l}
\text{Perm.:} \quad (1, 2, 3) \quad (1, 3, 2) \quad (2, 1, 3) \quad (2, 3, 1) \quad (3, 1, 2) \quad (3, 2, 1) \\
\text{Obs.:} \quad \begin{array}{cccccc}
\bullet & \bullet & \bullet & \bullet & \bullet & \bullet \\
\diagup & \diagdown & \diagdown & \diagup & \diagdown & \diagup \\
\bullet & \bullet & \bullet & \bullet & \bullet & \bullet \\
\diagdown & \diagup & \diagup & \diagdown & \diagup & \diagdown \\
\bullet & \bullet & \bullet & \bullet & \bullet & \bullet
\end{array}
\end{array} \quad (2)$$

For process monitoring, the online estimation of the OP series' current PMF vector is necessary. Weiß & Testik (2023) propose an EWMA approach for this purpose, namely by computing

$$\hat{\mathbf{p}}_{\pi,0} = \mathbf{p}_{\pi}^{(0)}, \quad \hat{\mathbf{p}}_{\pi,t} = \lambda \mathbf{Y}_t + (1 - \lambda) \hat{\mathbf{p}}_{\pi,t-1} \quad \text{for } t = 1, 2, \dots \quad (3)$$

Here, the binary vectors \mathbf{Y}_t of dimension $m! = 6$ are defined by the “one-hot encoding” $Y_{t,k} = \mathbb{1}(\pi_t = \pi^{[k]})$. The smoothing parameter $\lambda \in (0; 1)$ is chosen by the user, where the extent of smoothing and, thus, the inherent memory increases for decreasing λ . At each time t , the EWMA estimate $\hat{\mathbf{p}}_{\pi,t}$ is used to compute the value of the considered monitoring statistic, which is then plotted on a control chart and compared against the actual control limits (CLs).

In their research, Weiß & Testik (2023) compared six versions of such monitoring statistics. The three kinds of entropy-like statistics and resulting charts showed virtually the same performance, so it is sufficient to present only one of them here. As its statistic is most easily computed, we focus on the Δ_{π} -chart in the sequel, which plots the statistics

$$\hat{\Delta}_{\pi,t} = \sum_{k=1}^{m!} (\hat{p}_{\pi,t,k} - 1/m!)^2 \quad \text{for } t = 1, 2, \dots \quad (4)$$

against an upper CL (UCL) $l_{\Delta_{\pi}} > 0$. Among the remaining three charts in Weiß & Testik (2023), only the τ -chart and the β -chart showed an appealing performance. The τ -chart plots the statistics

$$\hat{\tau}_t = \hat{p}_{\pi,t,1} + \hat{p}_{\pi,t,6} - 1/3 \quad \text{for } t = 1, 2, \dots \quad (5)$$

against an UCL $l_{\tau} > 0$ and the corresponding lower CL (LCL) $-l_{\tau}$ (i. e., symmetric two-sided CLs), and the β -chart the statistics

$$\hat{\beta}_t = \hat{p}_{\pi,t,1} - \hat{p}_{\pi,t,6} \quad \text{for } t = 1, 2, \dots \quad (6)$$

against an UCL $l_{\beta} > 0$ and the corresponding LCL $-l_{\beta}$. These three control charts (4)–(6) shall serve as the competitors for our newly proposed control charts in Section 4 below. Since the charts are nonparametric, the actual values of the CL parameters $l_{\Delta_{\pi}}, l_{\tau}, l_{\beta}$ are unique across different marginal distributions of (X_t) , where the CL values for $\lambda \in \{0.25, 0.10, 0.05\}$ are summarized in Table 1 of Weiß & Testik (2023).

3 Review: Transcripts and Algebraic Distances

As said in Section 2, the permutations of $m \geq 2$ elements $\{1, 2, \dots, m\}$ (without restriction), endowed with function composition “ \circ ”, build a group called the symmetric group of degree m and denoted S_m . Among several possibilities, here we choose the one-line notation (i_1, i_2, \dots, i_m) for the permutation $n \mapsto i_n$ ($1 \leq n, i_n \leq m$); this notation will allow us below to leverage edit distances between permutations (viewed as strings of non-repeated symbols). Following the usual convention in the literature, the composition $\pi_1 \circ \pi_2$ of the permutations (or OPs for that matter) $\pi_1 = (i_1, i_2, \dots, i_m)$ and $\pi_2 = (j_1, j_2, \dots, j_m)$ is defined as a “right action”, meaning that the permutation π_1 acts first and π_2 acts second, i. e.,

$$\pi_1 \circ \pi_2 = (i_1, i_2, \dots, i_m) \circ (j_1, j_2, \dots, j_m) = (j_{i_1}, j_{i_2}, \dots, j_{i_m}). \quad (7)$$

To harness the algebraic structure of S_m in the analysis of time series symbolized with OPs, Monetti et al. (2009) introduced the concept of *transcript* between OPs. Specifically, given two OPs $\pi_1, \pi_2 \in S_m$, the transcript from the source π_1 to the target π_2 is the OP $\tau \in S_m$ defined as

$$\tau = \tau(\pi_1, \pi_2) := \pi_2 \circ \pi_1^{-1}. \quad (8)$$

The order of the source and target permutations matters because

$$\tau(\pi_2, \pi_1) = \pi_1 \circ \pi_2^{-1} = \tau(\pi_1, \pi_2)^{-1}. \quad (9)$$

For other properties of the transcripts, see Amigó et al. (2012).

As way of illustration, the composition (multiplication or Cayley) table $(\pi_i \circ \pi_j)_{1 \leq i, j \leq m}$ of the group S_3 is given by (see equation (7) with $m = 3$):

Composition \circ	$\pi^{[1]}$	$\pi^{[2]}$	$\pi^{[3]}$	$\pi^{[4]}$	$\pi^{[5]}$	$\pi^{[6]}$
$\pi^{[1]} = (1, 2, 3)$	$\pi^{[1]}$	$\pi^{[2]}$	$\pi^{[3]}$	$\pi^{[4]}$	$\pi^{[5]}$	$\pi^{[6]}$
$\pi^{[2]} = (1, 3, 2)$	$\pi^{[2]}$	$\pi^{[1]}$	$\pi^{[4]}$	$\pi^{[3]}$	$\pi^{[6]}$	$\pi^{[5]}$
$\pi^{[3]} = (2, 1, 3)$	$\pi^{[3]}$	$\pi^{[5]}$	$\pi^{[1]}$	$\pi^{[6]}$	$\pi^{[2]}$	$\pi^{[4]}$
$\pi^{[4]} = (2, 3, 1)$	$\pi^{[4]}$	$\pi^{[6]}$	$\pi^{[2]}$	$\pi^{[5]}$	$\pi^{[1]}$	$\pi^{[3]}$
$\pi^{[5]} = (3, 1, 2)$	$\pi^{[5]}$	$\pi^{[3]}$	$\pi^{[6]}$	$\pi^{[1]}$	$\pi^{[4]}$	$\pi^{[2]}$
$\pi^{[6]} = (3, 2, 1)$	$\pi^{[6]}$	$\pi^{[4]}$	$\pi^{[5]}$	$\pi^{[2]}$	$\pi^{[3]}$	$\pi^{[1]}$

(10)

Hence, the transcripts $\tau(\pi_1, \pi_2) = \pi_2 \circ \pi_1^{-1}$ for $\pi_1, \pi_2 \in S_3$ (see equation (8)) are given in the following table, where the source OP π_1 labels the rows (leftmost column) and the target OP π_2 labels the columns (topmost row):

Transcript τ	$\pi^{[1]}$	$\pi^{[2]}$	$\pi^{[3]}$	$\pi^{[4]}$	$\pi^{[5]}$	$\pi^{[6]}$
$\pi^{[1]} = (1, 2, 3)$	$\pi^{[1]}$	$\pi^{[2]}$	$\pi^{[3]}$	$\pi^{[4]}$	$\pi^{[5]}$	$\pi^{[6]}$
$\pi^{[2]} = (1, 3, 2)$	$\pi^{[2]}$	$\pi^{[1]}$	$\pi^{[5]}$	$\pi^{[6]}$	$\pi^{[3]}$	$\pi^{[4]}$
$\pi^{[3]} = (2, 1, 3)$	$\pi^{[3]}$	$\pi^{[4]}$	$\pi^{[1]}$	$\pi^{[2]}$	$\pi^{[6]}$	$\pi^{[5]}$
$\pi^{[4]} = (2, 3, 1)$	$\pi^{[5]}$	$\pi^{[6]}$	$\pi^{[2]}$	$\pi^{[1]}$	$\pi^{[4]}$	$\pi^{[3]}$
$\pi^{[5]} = (3, 1, 2)$	$\pi^{[4]}$	$\pi^{[3]}$	$\pi^{[6]}$	$\pi^{[5]}$	$\pi^{[1]}$	$\pi^{[2]}$
$\pi^{[6]} = (3, 2, 1)$	$\pi^{[6]}$	$\pi^{[5]}$	$\pi^{[4]}$	$\pi^{[3]}$	$\pi^{[2]}$	$\pi^{[1]}$

(11)

From equation (8), we conclude that the transcript $\tau(\pi_1, \pi_2)$ is the permutation τ that transforms π_1 into π_2 , in the sense that $\tau \circ \pi_1 = \pi_2$. Thus, it expresses a kind of “dissimilarity” between π_1 and π_2 , where $\pi^{[1]}$ corresponds to least dissimilarity according to (11). Therefore, it is not surprising that transcripts are related to the following two types of algebraic distance between two permutations (Amigó & Dale, 2025):

- (1) The *Cayley distance* $d_C : S_m \times S_m \rightarrow \{0, 1, \dots, m-1\}$ between $\pi_1, \pi_2 \in S_m$ is defined as the minimum number of transpositions needed to transform π_1 into π_2 . For example, $d_C((1, 2, 3), (3, 2, 1)) = 1$. It can be shown that

$$d_C(\pi_1, \pi_2) = m - C(\tau(\pi_1, \pi_2)), \quad (12)$$

where $C(\tau(\pi_1, \pi_2))$ is the number of cycles (including 1-cycles) in the cycle factorization of the transcript $\tau = \pi_2 \circ \pi_1^{-1}$ (Nguyen, 2024).

- (2) The *Kendall distance* $d_K : S_m \times S_m \rightarrow \{0, 1, \dots, m(m-1)/2\}$ between $\pi_1, \pi_2 \in S_m$ is defined as the minimum number of adjacent transpositions needed to transform π_1 into π_2 . For example, $d_K((1, 2, 3), (3, 2, 1)) = 3$. It can be shown that

$$d_K(\pi_1, \pi_2) = I(\tau(\pi_1, \pi_2)), \quad (13)$$

where $I(\tau(\pi_1, \pi_2))$ is the number of inversions in the transcript $\tau = \pi_2 \circ \pi_1^{-1}$, i. e., the number of ordered pairs (k_i, k_j) in $\tau = (k_1, \dots, k_m)$ such that $k_i > k_j$ (Kendall, 1938).

Equations (12) and (13) are used to compute the respective distances in practice. Note that (i) $d_C(\pi_1, \pi_2) \leq d_K(\pi_1, \pi_2)$ for all $\pi_1, \pi_2 \in S_m$, and (ii) the range of d_K is larger than the range of d_C except for $m = 2$ (in which case both ranges are $\{0, 1\}$). Therefore, we expect d_K to have more discrimination power in time series analysis than d_C . For other transcript-based tools in time series analysis, see Amigó & Dale (2026).

In the present research, we particularize the length of the OPs (and, hence, of the transcripts) and the algebraic distance, as follows.

Table 1: Possible 4-OPs obtained if a certain transcript is observed.

$\tau_t = \pi^{[1]}$	$\tau_t = \pi^{[2]}$	$\tau_t = \pi^{[3]}$	$\tau_t = \pi^{[4]}$	$\tau_t = \pi^{[5]}$	$\tau_t = \pi^{[6]}$
(1, 2, 3, 4)	(1, 2, 4, 3)	(2, 1, 3, 4)	(1, 4, 3, 2)	(1, 3, 2, 4)	(1, 3, 4, 2)
(4, 3, 2, 1)	(4, 3, 1, 2)	(3, 4, 2, 1)	(2, 1, 4, 3)	(1, 4, 2, 3)	(2, 4, 3, 1)
			(2, 4, 1, 3)	(2, 3, 1, 4)	(3, 1, 2, 4)
			(3, 2, 1, 4)	(2, 3, 4, 1)	(4, 2, 1, 3)
			(3, 2, 4, 1)	(3, 1, 4, 2)	
			(4, 1, 3, 2)	(3, 4, 1, 2)	
			(4, 2, 3, 1)	(4, 1, 2, 3)	

- The length of the OPs is $m = 3$ from now on. This is not only the most common length used in applications in general (Bandt, 2019), and for the control charts of Weiß & Testik (2023) in particular, recall Section 2, but it is also the length used in Weiß & Amigó (2026), some of whose results are instrumental for the present work. See (10) and (11) for the corresponding multiplication and transcript's tables.
- Weiß & Amigó (2026) also showed numerically that the Kendall distance d_K outperforms the Cayley distance d_C when it comes to detecting serial dependence in time series analysis. For this reason, we only use d_K for monitoring (in addition to the transcript series itself).

Thus, let (X_t) be a real-valued and continuously distributed process having a stationary OP-series (π_t) of length $m = 3$. The corresponding transcript series (τ_t) is defined by $\tau_t = \tau(\pi_t, \pi_{t+1}) := \pi_{t+1} \circ \pi_t^{-1}$ according to (8), and let $(d_{K,t})$ be the resulting series of Kendall distances, that is, $d_{K,t} = d_K(\pi_t, \pi_{t+1}) = I(\tau_t)$, see equation (13).

It should be noted, however, that for two consecutive OPs such as π_t and π_{t+1} in (τ_t) , some transitions are impossible, irrespective of the underlying process (X_t) . As summarized in Figure 1 of de Sousa & Hlinka (2022), it is impossible that $\pi^{[k]}$ with $k \in \{1, 3, 4\}$ is followed by $\pi^{[l]}$ with $l \in \{3, 4, 6\}$, and analogously with $k \in \{2, 5, 6\}$ and $l \in \{1, 2, 5\}$, where we took into account that de Sousa & Hlinka (2022) use different rules than ours to define and order the OPs. Altogether, each transcript τ_t corresponds to a set of possible 4-OPs of the vector $(x_t, x_{t+1}, x_{t+2}, x_{t+3})$, where $\tau_t = \pi_{t+1} \circ \pi_t^{-1}$, π_t is the 3-OP of (x_t, x_{t+1}, x_{t+2}) , and π_{t+1} is the 3-OP of $(x_{t+1}, x_{t+2}, x_{t+3})$; see Table 1 for a summary.

Let \mathbf{p}_τ be the stationary marginal distribution of the transcripts (τ_t) , i. e.,

$$\mathbf{p}_\tau = (p_{\tau;1}, \dots, p_{\tau;6})^\top := (P(\tau_t = \pi^{[1]}), \dots, P(\tau_t = \pi^{[6]}))^\top,$$

and \mathbf{p}_K the stationary marginal distribution of the Kendall distances, i. e.,

$$\mathbf{p}_K = (p_{K;0}, \dots, p_{K;3})^\top := (P(d_{K,t} = 0), \dots, P(d_{K,t} = 3))^\top.$$

To calculate \mathbf{p}_K from \mathbf{p}_τ , we need the following proposition (Weiß & Amigó, 2026).

3.1 Proposition *It holds:*

- (a) $d_K(\pi_1, \pi_2) = 0$ iff $\tau(\pi_1, \pi_2) = \pi^{[1]}$.
- (b) $d_K(\pi_1, \pi_2) = 1$ iff $\tau(\pi_1, \pi_2) \in \{\pi^{[2]}, \pi^{[3]}\}$.
- (c) $d_K(\pi_1, \pi_2) = 2$ iff $\tau(\pi_1, \pi_2) \in \{\pi^{[4]}, \pi^{[5]}\}$.
- (d) $d_K(\pi_1, \pi_2) = 3$ iff $\tau(\pi_1, \pi_2) = \pi^{[6]}$.

From Proposition 3.1, it follows that

$$\mathbf{p}_K = \mathbf{T}_K \mathbf{p}_\tau, \quad \text{where } \mathbf{T}_K = \begin{pmatrix} 1 & 0 & 0 & 0 & 0 & 0 \\ 0 & 1 & 1 & 0 & 0 & 0 \\ 0 & 0 & 0 & 1 & 1 & 0 \\ 0 & 0 & 0 & 0 & 0 & 1 \end{pmatrix}. \quad (14)$$

The following proposition (Weiß & Amigó, 2026) summarizes the relevant stochastic properties under the IC-assumption.

3.2 Proposition *Let (X_t) be i. i. d., so satisfying the IC-condition. Then, the transcripts' (τ_t) marginal distribution is given by*

$$\mathbf{p}_\tau^{(0)} = \frac{1}{24} (2, 2, 2, 7, 7, 4)^\top.$$

Furthermore, the Kendall distances $(d_{K,t})$ have the IC-marginal distribution

$$\mathbf{p}_K^{(0)} = \frac{1}{12} (1, 2, 7, 2)^\top \text{ with mean } \mu_K^{(0)} = \frac{11}{6}.$$

Note that the transcripts' IC-PMF, $\mathbf{p}_\tau^{(0)}$, simply agrees with the relative frequencies of the respective 4-OPs in Table 1.

4 Novel Control Charts based on Transcripts

Let (X_t) be the continuously distributed and real-valued process that is assumed to be i. i. d. under IC-conditions. Let (τ_t) be the corresponding series of transcripts, and $(d_{K,t})$ the series of Kendall distances. Recall from Proposition 3.2 that under IC-conditions, the transcripts' IC-distribution is given by $\mathbf{p}_\tau^{(0)} = \frac{1}{24} (2, 2, 2, 7, 7, 4)^\top$, and the one of the Kendall distances by $\mathbf{p}_K^{(0)} = \frac{1}{12} (1, 2, 7, 2)^\top$ with mean $\mu_K^{(0)} = \frac{11}{6}$. In analogy to equation (3), we first propose an EWMA-based online estimation with smoothing parameter $\lambda \in (0; 1)$ of the transcripts' current PMF vector, namely via

$$\hat{\mathbf{p}}_{\tau,1} = \mathbf{p}_\tau^{(0)}, \quad \hat{\mathbf{p}}_{\tau,t} = \lambda \mathbf{Z}_t + (1 - \lambda) \hat{\mathbf{p}}_{\tau,t-1} \quad \text{for } t = 2, 3, \dots \quad (15)$$

Here, the binary vectors \mathbf{Z}_t of dimension $m! = 6$ are again defined by a “one-hot encoding”, namely $Z_{t,k} = \mathbb{1}(\tau_t = \pi^{[k]})$. The corresponding online estimate of $d_{K,t}$ ’s PMF and mean follow from

$$\hat{\mathbf{p}}_{K,t} = \mathbf{T}_K \hat{\mathbf{p}}_{\tau,t} \quad \text{and} \quad \hat{\mu}_{K,t} = (0, 1, 2, 3) \hat{\mathbf{p}}_{K,t}, \quad (16)$$

respectively, recall (14). In view of the numerical experiments of Weiß & Amigó (2026) on hypothesis testing based on transcripts and algebraic distances, we now propose three novel types of control charts:

- the Δ_τ -chart plots the statistics

$$\hat{\Delta}_{\tau,t} = \sum_{k=1}^{m!} \frac{(\hat{p}_{\tau,t,k} - p_{\tau,k}^{(0)})^2}{p_{\tau,k}^{(0)}} \quad \text{for } t = 2, 3, \dots \quad (17)$$

against an UCL $l_{\Delta_\tau} > 0$;

- the Δ_K -chart plots the statistics

$$\hat{\Delta}_{K,t} = \sum_{i=0}^3 \frac{(\hat{p}_{K,t,i} - p_{K,i}^{(0)})^2}{p_{K,i}^{(0)}} \quad \text{for } t = 2, 3, \dots \quad (18)$$

against an UCL $l_{\Delta_K} > 0$;

- the μ_K -chart plots the statistics

$$\hat{\mu}_{K,t} = \hat{\mu}_{K,t} - 11/6 \quad \text{for } t = 2, 3, \dots \quad (19)$$

against an UCL $l_{\mu_K} > 0$ and LCL $-l_{\mu_K}$.

ARL computation and chart design of these charts are done by a simulation-based approach in analogy to Weiß & Testik (2023). Having specified a process model for (X_t) as well as a value for λ , one simulates the observations X_1, X_2, \dots and does an online computation of the considered chart statistic from (17)–(19). The time when the statistic first violates a CL is the run length of the control chart. These run length simulations are repeated for sufficiently many times (in this research, we always use 10^5 replications), and the sample mean across the replicated run lengths is an approximation of the control chart’s true (zero-state) ARL. For computing an IC-ARL, we benefit from the nonparametric nature of charts (17)–(19): as the marginal distribution is without effect on the charts’ IC-performances, we can simply use a normal distribution for simulation. Then, the actual chart design is determined iteratively; having specified a target value for the IC-ARL (in accordance to the SPM literature, we use the target $\text{ARL}_0 = 370$), one sets an initial value of the CL-parameter and determines the corresponding IC-ARL. If the deviation to ARL_0 is too large (in this research, we always tried to keep the absolute amount of deviation below 1), then the CL-value is revised and the IC-ARL is updated, and this procedure is repeated until a satisfactory chart design is achieved.

5 Performance Analyses

We analyze the performance of the newly proposed control charts (17)–(19) in comparison to the existing OP-EWMA charts surveyed in Section 2, where we use the simulation-based approach described at the end of Section 4 for ARL calculation and chart design. As the first step, we compute the required chart designs (i. e., the CLs of each chart) for achieving an IC-ARL close to $ARL_0 = 370$. As can be seen from Table 2, this was possible for any $\lambda \in \{0.25, 0.10, 0.05\}$ (ordered according to increasing memory), which are the same smoothing parameters as in Table 1 of Weiß & Testik (2023). Recall that the chart designs in Table 2 apply to any continuously-distributed process (X_t) due to the nonparametric nature of the charts (17)–(19). They can be immediately used in practice, irrespective of the IC-model’s marginal distribution and corresponding parametrization, and thus without the need for any parameter estimation.

Table 2: Chart designs (CL parameters $l_{\Delta_\tau}, l_{\Delta_K}, l_{\mu_K}$) for (17)–(19) and corresponding IC-ARLs for different values of smoothing parameter λ .

λ	Δ_τ -chart		Δ_K -chart		μ_K -chart	
	l_{Δ_τ}	ARL	l_{Δ_K}	ARL	l_{μ_K}	ARL
0.25	3.225	370.1	3.19	370.4	1.0188	369.8
0.10	0.9685	369.8	0.8078	369.7	0.5827	370.3
0.05	0.4328	370.2	0.3229	369.6	0.3785	370.5

Next, we use these chart designs for evaluating the OOC-performance of our novel control charts (17)–(19) in comparison to the existing charts (4)–(6) of Weiß & Testik (2023). Therefore, we simulated OOC-ARLs for various types of serially dependent data-generating process (DGP), thus violating the IC-assumption of (X_t) being i. i. d. Here, we consider all OOC-DGPs that were already considered by Weiß & Testik (2023). We show the corresponding OOC-ARLs of charts (4)–(6) in italic font for comparison, but we also complement our analyses by an additional DGP from Weiß & Amigó (2026), which is explained in more detail below.

The first OOC-DGP is the first-order autoregressive (AR(1)) process with i. i. d. innovations (ϵ_t) being standard-normally distributed,

$$X_t = \alpha X_{t-1} + \epsilon_t \quad \text{with } \epsilon_t \sim N(0, 1), \quad (20)$$

see Table 3 for the obtained OOC-ARLs. Note that Weiß & Testik (2023) omitted tabulating the OOC-ARLs of the β -chart (6), because this statistic is not sensitive towards the linear dependence implied by the AR(1) DGP. As AR(1) dependence is probably the most common type of serial dependence

Table 3: OOC-ARLs of novel control charts (17)–(19) compared to existing charts (4)–(5) for AR(1) DGP (20) with dependence parameter α and smoothing parameter λ . Italic numbers are taken from Weiß & Testik (2023). Lowest OOC-ARL among novel charts in bold font.

α	Δ_π	τ	Δ_τ	Δ_K	μ_K	α	Δ_π	τ	Δ_τ	Δ_K	μ_K
$\lambda = 0.25$											
0.2	<i>217.6</i>	<i>185.4</i>	210.2	212.1	181.1	-0.2	<i>640.2</i>	<i>798.2</i>	620.6	621.4	804.0
0.4	<i>128.5</i>	<i>101.8</i>	116.7	118.4	95.7	-0.4	<i>1162.0</i>	<i>1840.3</i>	808.3	795.1	1538.8
0.6	<i>75.3</i>	<i>60.4</i>	68.6	68.7	56.1	-0.6	<i>2266.1</i>	<i>4634.4</i>	449.9	432.2	969.6
0.8	<i>44.8</i>	<i>39.2</i>	42.3	42.7	35.6	-0.8	<i>5242.5</i>	<i>13649.7</i>	116.0	112.5	186.4
$\lambda = 0.10$											
0.2	<i>242.2</i>	<i>191.3</i>	233.8	200.6	171.4	-0.2	<i>531.3</i>	<i>411.2</i>	342.3	351.3	393.7
0.4	<i>152.9</i>	<i>99.9</i>	123.4	101.1	84.4	-0.4	<i>681.8</i>	<i>203.7</i>	175.5	153.4	155.8
0.6	<i>94.2</i>	<i>59.7</i>	68.3	57.5	49.5	-0.6	<i>565.1</i>	<i>83.8</i>	72.6	60.2	60.0
0.8	<i>57.6</i>	<i>40.5</i>	42.4	36.3	32.8	-0.8	<i>190.8</i>	<i>37.4</i>	32.3	27.6	28.7
$\lambda = 0.05$											
0.2	<i>269.5</i>	<i>206.2</i>	233.7	181.4	172.1	-0.2	<i>411.2</i>	<i>271.4</i>	264.9	274.4	246.5
0.4	<i>172.9</i>	<i>105.7</i>	117.5	88.0	82.4	-0.4	<i>326.2</i>	<i>118.0</i>	119.3	104.5	93.4
0.6	<i>108.7</i>	<i>63.8</i>	66.4	51.6	49.0	-0.6	<i>168.2</i>	<i>56.2</i>	55.7	46.6	44.3
0.8	<i>69.4</i>	<i>43.9</i>	43.2	34.8	33.7	-0.8	<i>71.3</i>	<i>30.7</i>	30.0	25.2	25.6

in practice, it is highly satisfactory to see that our novel control charts (especially the Δ_K - and μ_K -chart) show an appealing OOC-performance regarding both positive and negative serial dependence. For positive dependence, we see that the value of λ often has an only mild effect on the OOC-ARLs, and there is also not much difference between the different types of control charts. The μ_K -chart is always the best choice (but Δ_τ and Δ_K perform similarly well), and it always outperforms any of the existing charts of Weiß & Testik (2023). The situation of negative dependence is much more sophisticated. Here, large values of λ lead to a poor chart performance, with OOC-ARLs being sometimes much larger than the IC-ARLs (“biased ARL profile”). The best ARL performance is achieved for $\lambda = 0.05$, with again the μ_K -chart being the best overall solution. Hence, to sum up, the novel μ_K -chart clearly outperforms the existing OP-EWMA charts for both positive and negative AR(1) dependence, provided that $\lambda = 0.05$ in the latter case.

Next, we consider the transposed exponential AR(1) (TEAR(1)) process with standard-exponential i. i. d. innovations (ε_t), defined by

$$X_t = B_t^{(\alpha)} X_{t-1} + (1 - \alpha) \varepsilon_t \quad \text{with } \varepsilon_t \sim \text{Exp}(1), \quad (21)$$

where $(B_t^{(\alpha)})$ are i. i. d. Bernoulli random variables with $P(B_t^{(\alpha)} = 1) = \alpha$. The obtained OOC-ARLs are summarized in Table 4. The TEAR(1) DGP is quite demanding in a sense. On the one hand, its autocorrelation function

Table 4: OOC-ARLs of novel control charts (17)–(19) compared to existing charts (4)–(6) for TEAR(1) DGP (21) with dependence parameter α and smoothing parameter λ . Italic numbers are taken from Weiß & Testik (2023). Lowest OOC-ARL among novel charts in bold font.

α	Δ_π	β	τ	Δ_τ	Δ_K	μ_K
$\lambda = 0.25$						
0.1	<i>252.0</i>	<i>254.6</i>	<i>265.8</i>	264.6	267.0	257.8
0.2	<i>135.3</i>	<i>133.7</i>	<i>166.5</i>	156.5	158.2	157.8
0.3	<i>70.9</i>	<i>69.1</i>	<i>96.3</i>	86.1	87.2	90.4
0.4	<i>39.8</i>	<i>38.5</i>	<i>55.8</i>	49.1	49.9	51.9
0.5	<i>24.1</i>	<i>23.4</i>	<i>33.0</i>	29.3	29.8	31.0
0.6	<i>15.6</i>	<i>15.3</i>	<i>20.5</i>	18.4	18.7	19.3
$\lambda = 0.10$						
0.1	<i>238.4</i>	<i>231.1</i>	<i>286.0</i>	271.9	276.6	272.5
0.2	<i>115.5</i>	<i>108.8</i>	<i>191.0</i>	155.5	169.9	175.0
0.3	<i>59.2</i>	<i>55.1</i>	<i>113.6</i>	82.7	93.3	102.8
0.4	<i>34.4</i>	<i>32.0</i>	<i>65.1</i>	46.7	51.9	59.3
0.5	<i>22.1</i>	<i>20.6</i>	<i>38.3</i>	28.5	30.6	35.9
0.6	<i>15.3</i>	<i>14.5</i>	<i>23.6</i>	18.7	19.2	22.4
$\lambda = 0.05$						
0.1	<i>230.4</i>	<i>214.4</i>	<i>310.7</i>	265.3	284.0	290.4
0.2	<i>107.7</i>	<i>95.7</i>	<i>213.7</i>	143.5	177.0	188.5
0.3	<i>57.3</i>	<i>50.6</i>	<i>126.9</i>	77.2	97.9	110.2
0.4	<i>35.1</i>	<i>30.9</i>	<i>72.5</i>	45.9	54.9	64.2
0.5	<i>23.9</i>	<i>21.2</i>	<i>43.3</i>	29.8	32.8	39.2
0.6	<i>17.4</i>	<i>15.5</i>	<i>27.1</i>	20.6	20.9	25.3

(ACF) is exponentially decaying like in the AR(1) case, so it may be classified as being “linear” in this respect. On the other hand, it behaves highly asymmetric as the generated sample paths are characterized by long-lasting rises that are interrupted by abrupt falls. Recalling the definition of the 3-OPs in (2), it is clear that OP $\pi^{[1]} = (1, 2, 3)$ occurs much more frequently than $\pi^{[6]} = (3, 2, 1)$ (and also than the other OPs). Thus, the β -chart (6) is tailor-made for detecting this kind of dependence, which explains its superior performance in the analyses of Weiß & Testik (2023). From Table 4, we recognize that our novel control charts (17)–(19) do not reach this outstanding performance (with the Δ_τ -chart being the best among them), but they are at least competitive and better than the τ -chart of Weiß & Testik (2023).

The third OOC-DGP is the absolute AR(1) (AAR(1)) process defined by

$$X_t = \alpha |X_{t-1}| + \epsilon_t \quad \text{with } \epsilon_t \sim N(0, 1), \quad (22)$$

Table 5: OOC-ARLs of novel control charts (17)–(19) compared to existing charts (4)–(6) for AAR(1) DGP (22) with dependence parameter α and smoothing parameter λ . Italic numbers are taken from Weiß & Testik (2023). Lowest OOC-ARL among novel charts in bold font.

α	Δ_π	β	τ	Δ_τ	Δ_K	μ_K
$\lambda = 0.25$						
0.2	<i>329.6</i>	<i>334.0</i>	<i>326.6</i>	330.5	333.0	323.3
0.4	<i>237.8</i>	<i>252.9</i>	<i>229.0</i>	240.9	243.2	222.7
0.6	<i>147.0</i>	<i>169.9</i>	<i>132.0</i>	145.7	147.3	125.4
0.8	<i>79.3</i>	<i>101.7</i>	<i>68.1</i>	74.6	75.4	63.0
$\lambda = 0.10$						
0.2	<i>322.7</i>	<i>323.0</i>	<i>334.3</i>	329.8	336.6	329.3
0.4	<i>233.2</i>	<i>238.1</i>	<i>242.5</i>	245.2	243.9	224.4
0.6	<i>154.0</i>	<i>170.2</i>	<i>138.2</i>	149.2	135.9	119.5
0.8	<i>93.5</i>	<i>123.5</i>	<i>70.7</i>	76.1	65.8	58.1
$\lambda = 0.05$						
0.2	<i>320.5</i>	<i>313.1</i>	<i>346.5</i>	323.3	338.4	340.1
0.4	<i>234.1</i>	<i>224.7</i>	<i>264.3</i>	232.1	239.0	235.7
0.6	<i>160.7</i>	<i>164.9</i>	<i>150.4</i>	141.5	126.2	121.4
0.8	<i>104.7</i>	<i>136.6</i>	<i>76.0</i>	74.6	61.0	58.7

see Table 5 for the obtained OOC-ARLs. The process is nonlinear with an again asymmetric behavior, as the absolute value $|X_{t-1}|$ only leads to positive contributions. From Table 5, we recognize that the choice of λ is without a strong effect and that there is not much difference among the different control charts, similar to the classical AR(1) process (20) with positive α . In most cases, the μ_K -chart is superior among the novel charts, and it usually also outperforms all existing OP-EWMA charts.

A related OOC-DGP is the quadratic AR(1) (QAR(1)) process defined by

$$X_t = \alpha X_{t-1}^2 + \epsilon_t \quad \text{with } \epsilon_t \sim N(0, 1), \quad (23)$$

see Table 6, which is characterized by an analogous asymmetry as for the AAR(1) process (22), but with more pronounced positive shocks due to the squared term X_{t-1}^2 . Altogether, the QAR(1) process is highly nonlinear, but all charts from Table 5 are well-suited for detecting such kind of dependence. As before, we recognize only moderate differences between the different charts and different λ -values, where the μ_K -chart for $\lambda \geq 0.10$ and the Δ_τ -chart for $\lambda = 0.05$ are best among the novel control charts. They often also outperform the best OP-EWMA chart, or perform at least very similar to it.

While Weiß & Testik (2023) restricted their analyses to solely AR-type pro-

Table 6: OOC-ARLs of novel control charts (17)–(19) compared to existing charts (4)–(6) for QAR(1) DGP (23) with dependence parameter α and smoothing parameter λ . Italic numbers are taken from Weiß & Testik (2023). Lowest OOC-ARL among novel charts in bold font.

α	Δ_π	β	τ	Δ_τ	Δ_K	μ_K
$\lambda = 0.25$						
0.15	<i>283.8</i>	<i>290.3</i>	<i>285.1</i>	290.5	292.9	282.0
0.2	<i>219.3</i>	<i>230.5</i>	<i>217.2</i>	223.7	225.8	213.3
0.25	<i>116.0</i>	<i>123.8</i>	<i>114.9</i>	117.5	118.2	110.6
0.3	<i>35.7</i>	<i>37.6</i>	<i>35.5</i>	36.0	36.2	34.7
$\lambda = 0.10$						
0.15	<i>273.6</i>	<i>271.7</i>	<i>302.8</i>	286.6	297.2	288.4
0.2	<i>214.7</i>	<i>215.1</i>	<i>234.0</i>	224.8	228.4	218.8
0.25	<i>116.6</i>	<i>118.6</i>	<i>122.3</i>	119.8	118.6	113.2
0.3	<i>37.3</i>	<i>37.9</i>	<i>37.7</i>	37.6	36.3	35.9
$\lambda = 0.05$						
0.15	<i>268.8</i>	<i>254.3</i>	<i>321.9</i>	271.2	299.1	303.1
0.2	<i>213.6</i>	<i>200.4</i>	<i>257.8</i>	212.7	230.0	232.3
0.25	<i>120.0</i>	<i>113.6</i>	<i>134.3</i>	117.2	119.8	120.4
0.3	<i>39.5</i>	<i>38.3</i>	<i>40.7</i>	38.6	37.5	38.0

cesses, we follow Weiß & Amigó (2026) and also consider the first-order quadratic moving-average (QMA(1)) process, defined by

$$X_t = \epsilon_t + \beta \epsilon_{t-1}^2 \quad \text{with } \epsilon_t \sim N(0, 1), \quad (24)$$

as a further OOC-DGP. The (highly nonlinear and asymmetric) QMA(1) process is 1-dependent, which means that X_t and X_{t-h} are independent of each other for time lags $h \geq 2$. The rather large OOC-ARLs in Table 7 show that QMA(1) dependence is generally difficult to detect, where the Δ_τ -chart together with $\lambda = 0.05$ has the clearly best ARL performance among all novel charts. Its main competitor is the β -chart of Weiß & Testik (2023), also with $\lambda = 0.05$, which has a slightly lower OOC-ARL for the lowest dependence level $\beta = 0.2$, but is outperformed by the Δ_τ -chart otherwise.

In a nutshell, the newly proposed control charts (17)–(19), which are based on transcripts and algebraic distances, show an appealing ARL performance compared to the existing OP-EWMA charts (4)–(6) of Weiß & Testik (2023). In the case of the positively dependent AR-type processes, there is not much difference between the charts (17)–(19), and also the actual choice of λ has only little effect. These properties are attractive for the practitioner, as there is no “bad choice” regarding these types of dependence structure. If, in turn,

Table 7: OOC-ARLs of novel control charts (17)–(19) compared to existing charts (4)–(6) for QMA(1) DGP (24) with dependence parameter β and smoothing parameter λ . Lowest OOC-ARL among novel charts in bold font.

β	Δ_π	β	τ	Δ_τ	Δ_K	μ_K
$\lambda = 0.25$						
0.2	310.3	310.1	321.8	324.3	327.1	323.5
0.4	250.7	251.9	263.2	267.8	270.7	261.4
0.6	223.0	227.2	230.1	235.8	238.2	228.5
0.8	213.6	219.1	219.3	223.6	226.1	217.0
$\lambda = 0.10$						
0.2	277.5	272.9	334.6	286.3	317.4	323.6
0.4	213.2	207.2	281.1	215.1	253.4	261.1
0.6	200.7	193.3	248.3	192.8	219.8	228.7
0.8	204.4	195.0	238.5	190.5	208.8	219.3
$\lambda = 0.05$						
0.2	257.1	244.3	349.1	253.3	321.0	331.1
0.4	194.2	179.0	303.8	177.5	256.9	275.0
0.6	190.1	171.9	271.3	163.8	224.5	243.6
0.8	201.0	180.3	262.3	168.5	213.9	234.7

one is faced with possible negative AR(1) dependence or QMA(1) dependence, then the small smoothing parameter $\lambda = 0.05$ is clearly recommended, together with the μ_K -chart in the first case, and the Δ_τ -chart in the second case. Generally, one of these two charts, μ_K or Δ_τ , usually performed best among the novel charts (17)–(19), and except for the TEAR(1) process with its exceptional sample paths, they usually also outperform the OP-EWMA charts (4)–(6).

6 Illustrative Data Application

Inspired by the industrial application discussed in Weiß & Testik (2023), let us analyze the data set printed in Appendix A.3 of O’Donovan (1983, “Time series 4.1”), where the $n = 70$ consecutive yields from a batch chemical process as plotted in Figure 1 (a) are provided. Since our novel transcript-based charts (17)–(19) are nonparametric (similar to the former OP-EWMA charts of Weiß & Testik (2023)), they can immediately be applied to these data (using the chart designs from Table 2) without the need for any model fitting, in order to monitor the IC-assumptions of the batch yields being i. i. d. (irrespective of the actual marginal distribution). However, we can expect this IC-assumption to be violated, because batch data are known

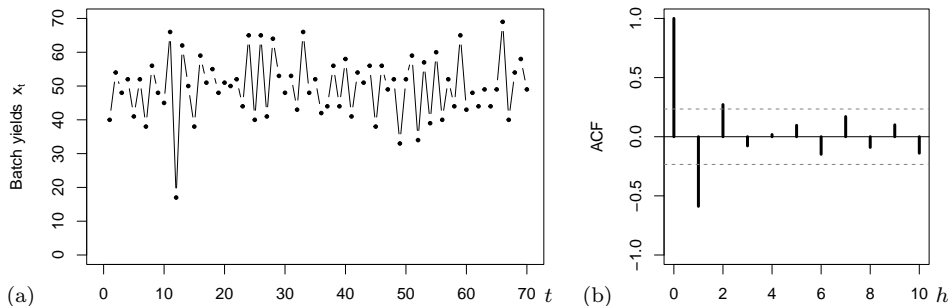


Figure 1: Chemical process data (x_t) of Section 6: (a) time series plot, and (b) plot of sample ACF against time lag h .

to commonly exhibit negative values for the ACF. According to O’Donovan (1983, p. 34), high-yielding batches often cause residues that reduce the yield of the respective subsequent batch, which explains the alternating behavior being visible in Figure 1 (a). In fact, the plotted sample ACF in Figure 1 (b) confirms this conjecture with a strongly negative lag-1 ACF of about -0.588 . Therefore, the OOC-ARL performance according to the right part of Table 3 (lines “ $\alpha = -0.6$ ”) appears to be a reasonable benchmark for interpreting the subsequent control charts.

We first applied our novel control charts (17)–(19) with $\lambda = 0.25$, but did not receive any alarm. This is plausible in view of the aforementioned Table 3, where the charts are not sensitive to negative dependence for such a large value of λ . However, we would expect a better OOC-performance if using $\lambda \leq 0.10$. This is confirmed by Figure 2, where all charts signal a violation of the IC-assumption. In fact, in agreement to Table 3, the charts with $\lambda = 0.05$ are faster in triggering their first alarm than those with $\lambda = 0.10$, and the μ_K -chart (19) is faster than the Δ_K -chart (18) and the Δ_τ -chart (17). The exact alarm times are

- $\lambda = 0.10$: $t = 26$ for Δ_τ , $t = 25$ for Δ_K , and $t = 24$ for μ_K ;
- $\lambda = 0.05$: $t = 25$ for Δ_τ , $t = 24$ for Δ_K , and $t = 23$ for μ_K .

Note that we express the alarm times in terms of the original sampling time according to Figure 2, in order to allow for a fair judgement: for computing the first k transcripts, we indeed have to collect $k + 3$ original observations, because the k th transcript is computed from the segment (x_k, \dots, x_{k+3}) .

Finally, we also applied the OP-EWMA charts from Section 2 for comparison. More precisely, as already explained for Table 3, the β -chart is not useful for linear dependence, so we focus on the OP-EWMA charts (4) and (5) of Weiß & Testik (2023) as the competitors. Here, the Δ_π -chart (4) does not trigger an alarm at all for $\lambda \geq 0.10$, and only at $t = 62$ for $\lambda = 0.05$. This poor performance appears reasonable in view of Table 3. It is also

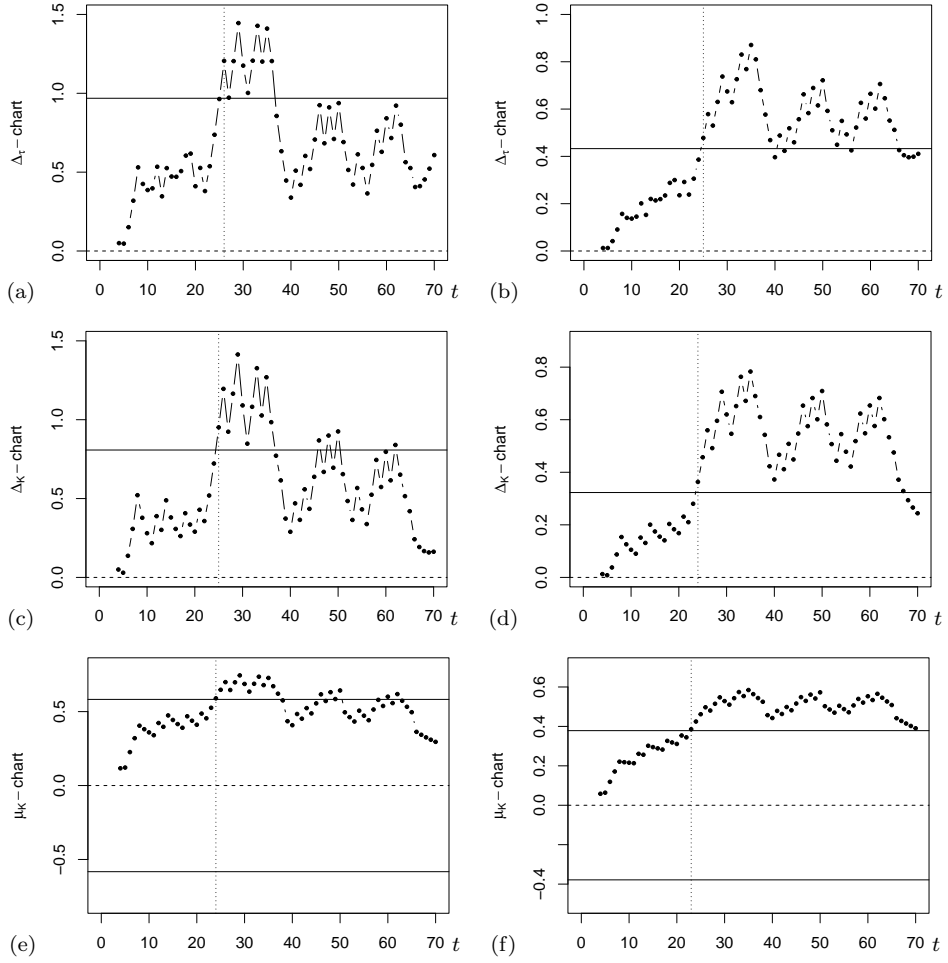


Figure 2: Chemical process data (x_t) of Section 6: Δ_τ -, Δ_K -, and μ_K -charts for $\lambda = 0.10$ (left column) and $\lambda = 0.05$ (right column).

reasonable that the τ -chart (5) is much faster, namely $t = 26$ if $\lambda = 0.10$ and $t = 24$ if $\lambda = 0.05$. But altogether, τ is outperformed by Δ_K and μ_K , in agreement to our findings from Table 3. So we confirm the appealing performance of our novel transcript-based control charts.

7 Conclusions

The topic of this article is the application of transcripts to control charts, i. e., to the detection of change points regarding serial dependence in (continuously distributed) stochastic processes (X_t). The context is the analysis of time series in ordinal representations, meaning symbolic representations whose symbols (OPs) can be viewed as permutations. In comparison to

Weiß & Testik (2023), where OPs were used to the same end, here, we go further and exploit two important features of permutations.

- (1) **The algebraic structure.** Permutations on m objects, endowed with function composition “ \circ ”, build the symmetric group S_m of degree m . This algebraic structure allows to define the concept of transcript from $\pi_1 \in S_m$ to $\pi_2 \in S_m$ as $\tau(\pi_1, \pi_2) = \pi_2 \circ \pi_1^{-1} \in S_m$, which is a generalization of the concept of difference in additive groups. In this paper, we focus on the case $m = 3$.
- (2) **The metric structure.** Permutations on m objects build a metric space, too. In Section 3, we present two algebraic distances in S_m : the Cayley distance d_C and the Kendall distance d_K . As it turns out, both $d_C(\pi_1, \pi_2)$ and $d_K(\pi_1, \pi_2)$ can be easily calculated from the transcript $\tau(\pi_1, \pi_2)$; see equations (12) and (13). In this paper, we only use the Kendall distance due to its better performance in previous works.

With these two tools of ordinal representations at hand — transcripts and transcript-based distances — we proceed as follows. The real-valued process (X_t) is converted (in an online manner) into, first, an OP-valued process (π_t) (Section 2), and second, into the OP-valued process $(\tau_t) = (\tau(\pi_t, \pi_{t+1}))$. Then, one monitors statistical properties (in particular, serial dependence) of the process (X_t) via (τ_t) and/or the integer-valued process $(d_{K,t}) = (d_K(\pi_t, \pi_{t+1}))$.

We apply the above approach to control charts in Sections 4–6, the in-control assumption (“null hypothesis”) being that (X_t) is i. i. d. To monitor for dependence changes in (X_t) , in Section 4, we propose three novel, transcript-based and nonparametric control charts: the Δ_τ -chart (17), the Δ_K -chart (18), and the μ_K -chart (19). Their ARL performance is compared to that of the existing OP-EWMA charts (4)–(6) using different serially dependent processes (equations (20)–(24)) in Section 5. The same methodology is applied in Section 6, this time to real-world data. There, consecutive yields from a batch chemical process are monitored, with batch data being known to generally exhibit negative values of the ACF. The numerical simulations in Section 5 show a very satisfactory performance of the novel nonparametric control charts. Altogether, the best performers are the charts μ_K and Δ_τ . These positive outcomes are also confirmed by the chemical process data in Section 6, with Δ_K and μ_K now offering the best performance. In view of the above encouraging results, we conclude that the transcript-based control charts Δ_τ , Δ_K , and μ_K are useful for a nonparametric monitoring of serial dependence.

Future research will explore the possibility of extending our transcript-based approach to monitoring spatial OPs like in Adammer et al. (2026).

References

- Adammer, P., Wittenberg, P., Wei, C.H., Testik, M.C. (2025) Nonparametric monitoring of spatial dependence. *Technometrics* **68**(2), 267–281.
- Alwan, L.C. (1992) Effects of autocorrelation on control chart performance. *Communications in Statistics — Theory and Methods* **21**(4), 1025–1049.
- Amig, J.M., Monetti, R., Aschenbrenner, T., Bunk, W. (2012) Transcripts: An algebraic approach to coupled time series. *Chaos: An Interdisciplinary Journal of Nonlinear Science* **22**(1), 013105.
- Amig, J.M., Dale, R. (2025) Permutation-based distances for groups and group-valued time series. *Entropy* **27**(9), 913.
- Amig, J.M., Dale, R. (2026) Entropic and algebraic transcript-based tools in time series analysis *Chaos: An Interdisciplinary Journal of Nonlinear Science* **36**(5), 053103.
- Atienza, O.O., Tang, L.C., Ang, B.W. (1997) ARL properties of a sample autocorrelation chart. *Computers and Industrial Engineering* **33**(3–4), 733–736.
- Bandt, C., Pompe, B. (2002) Permutation entropy: a natural complexity measure for time series. *Physical Review Letters* **88**(17), 174102.
- Bandt, C. (2019) Small order patterns in big time series: a practical guide. *Entropy* **21**(6), 613.
- Berger, S., Kravtsiv, A., Schneider, G., Jordan, D. (2019) Teaching ordinal patterns to a computer: efficient encoding algorithms based on the Lehmer code. *Entropy* **21**(10), 1023.
- Chakraborti, S., Graham, M.A. (2019) Nonparametric (distribution-free) control charts: An updated overview and some results. *Quality Engineering* **31**(4), 523–544.
- Chakraborti, S., Sparks, R.S. (2020) Statistical process monitoring and the issue of assumptions in practice: normality and independence. In Koutras & Triantafyllou (eds.): *Distribution-Free Methods for Statistical Process Monitoring and Control*, Springer Nature Switzerland AG, Cham, 137–155.
- Kendall, M.G. (1938) A new measure of rank correlation. *Biometrika* **30**(1/2), 81–93.
- Koutras, M.V., Triantafyllou, I.S. (2020) Recent advances on univariate distribution-free Shewhart-type control charts. In Koutras & Triantafyllou

- (eds.): *Distribution-Free Methods for Statistical Process Monitoring and Control*, Springer Nature Switzerland AG, Cham, 1–56.
- Machado, J.A.F., Santos Silva, J.M.C. (2005) Quantiles for counts. *Journal of the American Statistical Association* **100**(472), 1226–1237.
- Monetti, R., Bunk, W., Aschenbrenner, T., Jamitzky, F. (2009) Characterizing synchronization in time series using information measures extracted from symbolic representations. *Physical Review E* **79**(4), 046207.
- Montgomery, D.C. (2009) *Introduction to Statistical Quality Control*. 6th edition, John Wiley & Sons, Inc., New York.
- Nguyen, T. (2024) Improving the Gilbert–Varshamov bound for permutation codes in the Cayley metric and Kendall τ -metric. *arXiv preprint* 2404.15126v2.
- O’Donovan, T.M. (1983) *Short Term Forecasting: An Introduction to the Box–Jenkins Approach*. John Wiley & Sons, Chichester.
- Olmstead, P.S. (1967) Our debt to Walter Shewhart. *Industrial Quality Control* **24**(2), 72–73.
- de Sousa, A.M.Y.R., Hlinka, J. (2022) Assessing serial dependence in ordinal patterns processes using chi-squared tests with application to EEG data analysis. *Chaos: An Interdisciplinary Journal of Nonlinear Science* **32**(7), 073126.
- Wardell, D.G., Moskowitz, H., Plante, R.D. (1992) Control charts in the presence of data correlation. *Management Science* **38**(8), 1084–1105.
- Weiß, C.H., Amigó, J.M. (2026) Transcripts and algebraic distances in time series: Stochastic properties and nonparametric dependence tests. *arXiv preprint* 2605.25478.
- Weiß, C.H., Schnurr, A. (2024) Generalized ordinal patterns in discrete-valued time series: nonparametric testing for serial dependence. *Journal of Nonparametric Statistics* **36**(3), 573–599.
- Weiß, C.H., Testik, M.C. (2023) Non-parametric control charts for monitoring serial dependence based on ordinal patterns. *Technometrics* **65**(3), 340–350.
- Yourstone, S.A., Montgomery, D.C. (1989) A time-series approach to discrete real-time process quality control. *Quality and Reliability Engineering International* **5**(4), 309–317.